Translational Predictive Biomarker Analysis of the Phase 1b Sorafenib and Bevacizumab Study Expansion Cohort*

Nilofer Azad[a,b,c], Minshu Yu[a,b], Ben Davidson[d,e], Peter Choyke[f], Clara C. Chen[g], Bradford J. Wood[h], Aradhana Venkatesan[h], Ryan Henning[a,i], Kathy Calvo[j], Lori Minasian[a], Daniel C. Edelman[k], Paul Meltzer[k], Seth M. Steinberg[l], Christina M. Annunziata[a], and Elise C. Kohn[a,m]

Predictive biomarkers are needed to triage patients to the best therapy. We prospectively planned examination of sequential blood, biopsy, and functional imaging with which to confirm the mechanism and to identify potential predictive biomarkers in a phase Ib clinical trial expansion of patients with solid tumors receiving sorafenib/bevacizumab. The maximally tolerated doses of sorafenib at 200 mg twice daily with bevacizumab at 5 mg/kg every other week were given to biopsiable patients. Patients were randomized to receive either sorafenib or bevacizumab monotherapy for the first 28-day cycle with the second drug added with cycle 2. Biopsies, dynamic contrast-enhanced MRI, and fluorodeoxyglucose-proton emission tomography were done pre-therapy and at 2 and 6 weeks (2 weeks into combination therapy). Tumor and serum proteomics, Ras/Raf mutational analysis, and functional imaging results were examined individually and across the dataset to identify potential changes predictive of response to therapy and those that confirm the biochemical drug mechanism(s). Therapy with sorafenib/bevacizumab resulted in clinical benefit in 45% of this mixed solid tumor group. ERK activation and microvessel density were decreased with monotherapy treatment with sorafenib or bevacizumab, respectively; whereas a decreased signal over the group of total AKT, phospho(p)-VEGF receptor2, p-endothelial nitric-oxide synthase, b-RAF, and cleaved poly(ADP-ribose) polymerase was associated with earlier progression of disease. Tumor metabolic activity decreased in those patients with clinical benefits lasting longer than 4 months, and activity increased with progression of disease. Cleavage of caspase 3 and poly(ADP-ribose) polymerase was increased, and Ki67 expression decreased in patients with prolonged clinical benefits, consistent with decreased proliferation and increased apoptosis. The conglomerate analysis, incorporating pharmacodynamic and tumor biochemistry, demonstrated sorafenib/bevacizumab-targeted vascular activity in the tumor. Results suggest potential biomarkers for which changes, as a group, during early therapeutic exposure may predict clinical benefit. ***Molecular & Cellular Proteomics 12: 10.1074/mcp.M112.026427, 1621–1631, 2013.***

Sorafenib and bevacizumab have demonstrated clinical utility as single agents or in combination with chemotherapy for solid tumors. Sorafenib, initially developed as a c-Raf kinase inhibitor, also has potent inhibitory activity against the vascular endothelial growth factor receptor-2 (VEGFR2).[1] Clinical activity has been shown for bevacizumab, the humanized neutralizing monoclonal antibody against VEGF, also alone and in chemotherapy combinations (1–5). The role of combining two agents with overlapping target biology had not yet been studied.

We tested the clinical hypothesis that signal interruption at collaborative pathway points, both vertical and horizontal interactions, may yield equal or greater effect than the agents in isolation in a phase I trial combining bevacizumab and sorafenib (NCT00095459), and we now report the translational analyses (6). Sorafenib was selected for its ability to target

From the [a]Medical Oncology Branch, [c]Sidney Kimmel Comprehensive Cancer Center at Johns Hopkins, 1650 Orleans St., Rm. 4M10, Baltimore, Maryland 21231, [d]Division of Pathology, Norwegian Radium Hospital, Oslo University Hospital, and Institute for Clinical Medicine, Faculty Division Radiumhospitalet, the Medical Faculty, University of Oslo, Oslo, Norway, [f]Molecular Imaging Program, [g]Division of Nuclear Medicine, Radiology, and Imaging Sciences and [h]Center for Interventional Oncology, Radiology, and Imaging Sciences, Clinical Center, National Institutes of Health, Bethesda, Maryland 20892, [j]Laboratory of Pathology, and the [k]Genetics Branch, and [l]Biostatistics and Data Management Section, Center for Cancer Research, NCI, National Institutes of Health, Bethesda, Maryland 20892

Received December 12, 2012, and in revised form, February 20, 2013

Published, MCP Papers in Press, February 28, 2013, DOI 10.1074/mcp.M112.026427

[1] The abbreviations used are: VEGFR2, vascular endothelial growth factor receptor-2; RPPA, reverse phase proteomic array; FDG-PET, fluorodeoxyglucose-proton emission tomography; DCE-MRI, dynamic contrast-enhanced magnetic resonance imaging; PARP, poly-(ADP-ribose) polymerase; MR, magnetic resonance; GKM, general kinetic Kety model; SUV, small unilamellar vesicle; HR, hazard ratio; PR, partial response; PD, progressive disease; SD, stable disease; PFS, progression free survival.

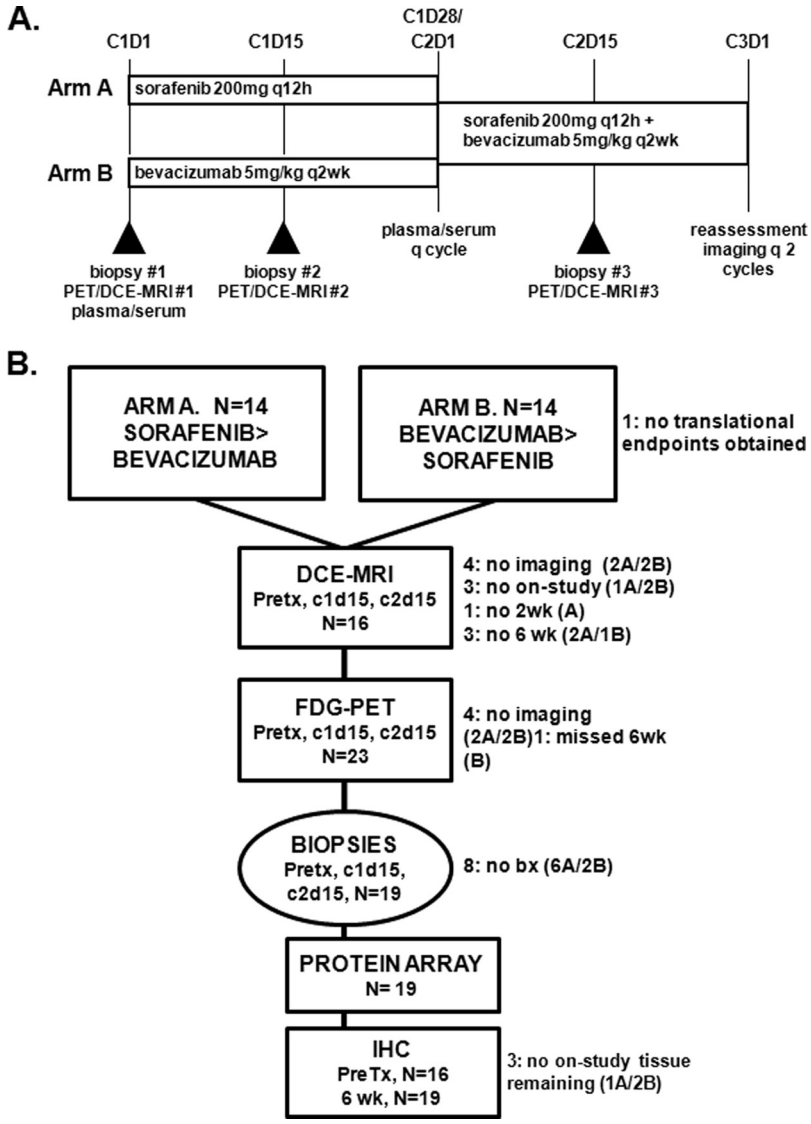

FIG. 1. **Treatment schema (*A*) and Consort diagram (*B*).**

both receptor and cytosolic kinases important in a variety of activated cells in the tumor microenvironment, including stromal, endothelial, and malignant cells. Because such kinase inhibitor treatment has been shown to up-regulate production of proangiogenic cytokines, we added bevacizumab to reduce VEGF ligand availability and augment inhibition of endothelial cells. We observed the clinical benefit, including partial response and prolonged disease stabilization, using attenuated doses of the individual agents as determined by safety assessments during the trial; partial response or disease stabilization of at least 4 months occurred in 59% of the daily sorafenib cohort and in 55% of those on the intermittent, 5 of 7 days, sorafenib schedule (6, 7). These benefits lasted up to 37+ months with over 25% of patients receiving 12 or more months of therapy. The trial prospectively planned comprehensive translational assessment using a randomized drug addition design (Fig. 1*A*) to evaluate individual drug target specificity and combination drug effects to identify potential predictive biomarkers to examine in the ongoing phase II study of sorafenib/bevacizumab in ovarian cancer.

Predictive biomarkers are increasingly important for the advancement of targeted therapies. Such knowledge should allow more effective triage of patients to interventions more likely to provide clinical benefit. Biomarkers that predict drug response may consist of direct measures of activity, such as modulation of biochemical signals in the tumor (8) or those that yield pharmacodynamic measures, such as functional imaging (9, 10). Changes in metabolic activity and/or blood flow using dynamic imaging may fall into both categories with decreased glucose uptake due to reduced glucose delivery and/or reduced glucose metabolism and altered vascular permeability in response to attenuation of the VEGF drive. Aggregate analysis of these varied translational measures may yield a more detailed view of the cancer and the drug combination, allowing broader dissection into potential predictive

biomarkers. Linking modulation of activity with clinical benefit is a first step in validating prospective biomarkers.

We designed a novel drug administration schema from which to examine the contribution of both sorafenib and bevacizumab on the modulation of tumor and the tumor microenvironment behavior. The biochemical and imaging data demonstrate changes consistent with alteration of tumor vascularity, demonstrate direct association of target effect with clinical outcome across solid tumor types, and confirm the benefit of complementary pathway targeting. Reduction in blood flow, up-regulation of cytokine production, and inhibition of a set of anti-apoptotic anti-proliferative signaling events together may define potentially predictive changes to examine in early drug administration in subsequent trials.

EXPERIMENTAL PROCEDURES

Patients and Samples

—Details of the NCI IRB-approved phase I study and expansion cohort have been published previously (6). The maximally tolerated dose, 200 mg of sorafenib twice daily and 5 mg/kg bevacizumab every 2 weeks in 28-day cycles, was administered in this expansion cohort in a novel randomization schema (Fig. 1*A*; one additional patient was enrolled after submission of the phase I report). Blood samples were obtained, processed, and stored within 4 h of sampling (6). Peripheral blood mononuclear cells were collected once for mutational analyses, and serum and plasma were collected monthly. Patients underwent elective image-guided percutaneous 18-gauge core needle biopsy, under separate informed consent and local anesthesia, by an interventional radiologist. Tissue samples were frozen immediately in OCT in the interventional radiologist suite and stored at −80 °C until analysis. If the quality of the initial biopsy was poor or tumor was lacking, subsequent biopsies were aborted per protocol.

Functional Imaging

Dynamic Contrast Enhanced Magnetic Resonance (MR)—All MR images were obtained at base line and at protocol-defined points. Region-of-interest MR measurements were obtained from one selected target lesion, independent of the biopsy site, from scans within 48 h prior to each of the three biopsies. Imaging was performed on a 1.5-T MR system (GE Healthcare or Philips Achieva, Best, The Netherlands) using dedicated receive-only phased array coils. Continuous 30-s imaging data sets were obtained before, during, and after administration of the contrast medium for a total of 8 min, resulting in 23 repeated datasets. T2-weighted images (time of repetition (TR)/time of echo (TE) 4600/100 ms, a section thickness of 6 mm, 400-mm field of view, and a matrix of 320 × 320) were used to locate the target tumor. Next, unenhanced T1-weighted images (TR/TE 9/3.6 ms, a 5° flip angle, 5-mm-thick sections, 400-mm field of view, and a matrix of 256 × 256) were obtained with a three-dimensional spoiled gradient-echo sequence to determine the tissue T1 map. Finally, DCE-MR images (TR/TE 9/3.6 ms, a 15° flip angle, 5-mm-thick sections through the entire target lesion, 400-mm field of view, an acquisition time of 30 s per data set, and a matrix of 256 × 256) were obtained with a three-dimensional spoiled gradient-echo sequence. After three base-line unenhanced image acquisitions, an automatic injector (Medrad Spectris, Indianola, PA) was used to intravenously infuse gadopentetate dimeglumine (Magnevist; Bayer Healthcare Pharmaceuticals, Wayne, NJ) at 0.3 ml/s, for a total of 0.1 mmol/kg of body weight (typically 15–20 ml), followed by a 50-ml normal saline flush.

DCE-MR Image Analysis—MR data were analyzed using a two-compartment model based on the general kinetic (GKM) Kety model (11, 12). Three parameters derived from the curve-fitting GKM algorithm were used to generate quantitative parameters as follows: K_{trans}, the forward contrast transfer rate; k_{ep}, the reverse contrast transfer rate; V_e, extravascular, extracellular volume fraction of the tumor. The DCE-MRI model incorporates an arterial input function derived from large arteries (*e.g.* aorta) and a T1 map for converting signal intensity to gadolinium concentration. It is based on a two-compartment model that assumes that the vascular space is in rapid equilibrium with the extravascular, extracellular space, and it further assumes a rapid water exchange between intra- and extracellular water. The GKM model was programmed in an IDL-based (Interactive Data Language; Research Systems Inc., Boulder, CO) research tool (Cine Tool, GE Healthcare).

FDG-PET—Patients fasted at least 6 h prior to the intravenous injection of [^{18}F]fluorodeoxyglucose (15 mCi). Emission images (8 min) were obtained in two-dimensional mode from the upper thigh to the base of skull starting ~60 min after injection. Transmission scans (3 min) were obtained for attenuation correction. Scans were performed using a GE Advance scanner (General Electric Medical Systems) with a 15-cm axial field of view. PET images were reconstructed on a 256 × 256 matrix using an iterative algorithm provided by the manufacturer. SUV values corrected for lean body mass were obtained using the maximum pixel activity value within a region of interest drawn over index lesions. Index lesions assessed on MR were identified and SUV measurements performed.

Protein Analysis and Quantitation

Immunohistochemistry—Serial frozen sections for the set of three time points were fixed in acetone and incubated with primary antibody (Table I). CD31-stained slides were pre-heated in a microwave oven for 5 min; no other antigen retrieval was done. Visualization was achieved using the Dako EnVision™+ peroxidase system. Appropriate positive and negative controls were included in each staining experiment, and all specimens containing <100 tumor cells were excluded. Staining was considered positive when localized to the nucleus (Ki-67 and p85-PARP) or cytoplasm (VEGF, CD31, and p85-PARP). Staining extent was scored blinded by a gynecopathologist (BD Biosciences) for the number of positive cells on a scale of 0–4 for Ki-67, p85-PARP, and VEGF as follows: 0 = no staining, 1 = 1–5%, 2 = 6–25%, 3 = 26–75%, and 4 = 76–100% of tumor cells (13). CD31-positive vessels are presented as the average number of vessels per 10 high power fields (×400 magnification).

RPPA—Tissue quantity assessment and quantitation, lysis, serial dilution, and antibody analysis was done according to our optimized procedure (14). The core from each biopsy set with the greatest percentage of tumor, and the least necrosis was selected for use after biopsy pathology was reviewed (Fig. 2), and tissue area was measured using the Veritas laser capture microdissection system (Arcturus, Sunnyvale, CA). Final tissue quantity was 8 μm × 30 mm^2, which approximated 30 μg of total tissue. Two independent replicate tissue sample sets from each set of biopsies were used. Lysates were randomly distributed onto the RPPA slides in triplicate, undiluted and serially diluted 1:2, on 40 replicate nitrocellulose membrane-coated slides (Whatman) by an Aushon 2470 arrayer (Aushon, Billerica, MA).

Internal controls included lysates from human microvascular endothelial cells, HeLa cells, and A431 cells treated with growth factors or apoptosis-inducing agents (15) as follows: human microvascular endothelial cells ± VEGF (50 ng/ml for 2 min); HeLa cells ± etoposide (25 μM for 5 h), or EGF (100 ng/ml for 2 h), and untreated A431 cells for vascular cell activation, apoptosis, and receptor tyrosine kinase pathway activation, respectively. A sample buffer-only negative control was printed with each dilution replicate for ambient background.

Target proteins were detected by specific validated antibodies from the same lot tested for validation and optimization (Table I),

TABLE I
Antibodies and titers used for immunohistochemistry (IHC) and RPPA

Antigen	Source	Catalog no.	Type and dilution for IHC
VEGF	Dako, Glostrup, Denmark	M7273	Murine mAb* 1:25
CD31	Dako, Glostrup, Denmark	M0823	Murine mAb 1:80
Proliferating cell nuclear antigen	Dako, Glostrup, Denmark	M7240	Anti-Ki-67 mAb 1:50
p85-cleaved PARP	Promega, Madison, WI	G7341	Rabbit polyclonal 1:100
Antigen	**Source**	**Catalog no.**	**Type and dilution for RPPA**
AKT	Cell Signaling	2694	Polyclonal Ab 1:500
P473Ser-AKT	Cell Signaling	9271	Polyclonal Ab 1:500
ERK	Cell Signaling	9102	Polyclonal Ab 1:500
P202Thr/204Tyr-ERK	Cell Signaling	4377	mAb 1:1000
EGF receptor	Cell Signaling	4405	mAb 1:200
P845Tyr-EGF receptor	Cell Signaling	2231	Polyclonal Ab 1:200
VEGFRII	Cell Signaling	2479	mAb 1:500
PTyr1175-VEGFRII	Cell Signaling	2478	mAb 1:1000
B-Raf	Cell Signaling	9433	mAb 1:1000
P1177Ser-eNOS	Cell Signaling	9570	mAb 1:1000
P38	Abcam	ab7952	Polyclonal Ab 1:1000
Cleaved caspase 3	Cell Signaling	9661	Polyclonal Ab 1:1000
Cleaved PARP	Cell Signaling	9541	Polyclonal Ab 1:1000

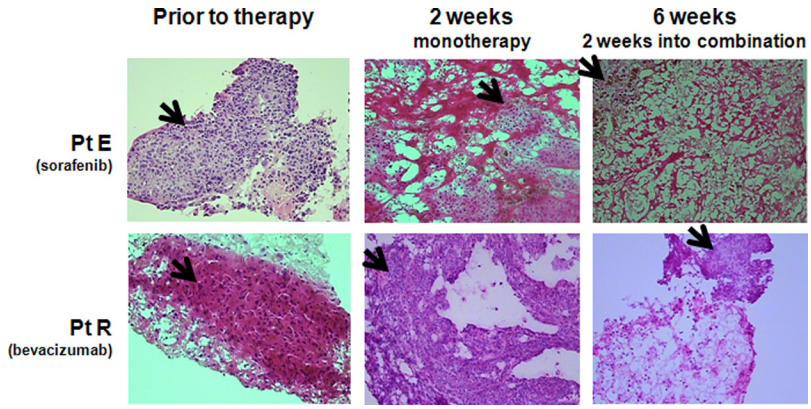

FIG. 2. **Example of core needle biopsy specimens.** Representative 18-gauge core needle biopsy specimens pre-treatment, after 2 weeks of monotherapy, and at 6 weeks is shown. Patient E (*Pt E*) received sorafenib for cycle 1 monotherapy and patient R (*Pt R*) received bevacizumab monotherapy on cycle 1. Slides are stained with H&E, and this is a Veritas laser capture microdissection digital picture taken during tissue assessment and measurement. *Arrows* point to areas of viable tumor.

using an avidin-biotin amplification system and stained with diaminobenzidine (DAKO, Carpinteria, CA). Colloidal gold stain (Bio-Rad) was used to quantitate total protein load per spot. Stained slides were scanned; spot intensity was measured, and intensity values were normalized to total protein as described (14).

Mutational Analysis

For DNA extraction, 8-μm tissue recuts, providing a total area of 10–20 mm^2, were provided to the Clinical Molecular Profiling Core, Genetics Branch, Center for Cancer Research, NCI, National Institutes of Health (DA). OCT was removed by washing samples in 500 μl of TE and centrifuging the tissue for 10 min (500 $\times$ *g*). DNA was then extracted from the tissues with the QIAamp DNA Micro Kit (Qiagen, Valencia, CA). Mutational analysis was done using standard Sanger DNA sequencing protocols after amplification and applied M13-tagged primers against all exons in *BRAF*, *KRAS*, *NRAS*, and *HRAS*. Amplicons were evaluated by gel electrophoresis, cleaned (Exo-Sap It; United States Biochemical Corp., Cleveland, OH), and then sequenced using BigDye® terminator version 3.1 cycle sequencing kit (Applied Biosystems). GenBank™ reference sequences NM_004333.4, NM_033360.2, NM_002524.3, and NM_005343.2, respectively, were used in the DNA sequence analysis (Mutation Surveyor software, Softgenetics, State College, PA) with default settings. Single nucleotide polymorphisms without commensurate amino acid change did not require repeat sequencing, although base pair changes resulting in a mutant protein underwent repeat sequencing for confirmation.

Statistical Considerations

Ten patients per arm, each with three sequential usable biopsies, were needed to provide 80% power to detect a difference equal to 1.5 S.D. of the change from base line for eight primary parameters with an

TABLE II
Patient demographics

Male/Female	10:18
Median age	58.4 (30.3–76)
Tumor types	
Ovarian/fallopian/peritoneal	7
Melanoma	5
Sarcoma	5
Other[a]	11
Median 28 day cycles on therapy	4.75 (0.5–36.5)
Best response	
Partial response	5
Stable disease	19
Progressive disease	3
Not evaluable	1

[a] Other includes the following: adrenocortical, papillary renal cell, cervical, colon, peritoneal mesothelioma, uterine papillary serous, unknown primary, papillary thyroid, rectal squamous, adenoid cystic breast, and granulosa cell cancers (one each).

overall $\alpha = 0.05$ per arm. All results are considered exploratory and all tests used nonparametric statistics, with a Hochberg adjustment for multiple comparisons. Relative changes from base line or from week 2 were used in the analyses, as these were less dependent on the earlier time point values than were absolute changes. Continuous data between the two groups were examined with an exact Wilcoxon rank sum test. Spearman correlation analysis determined the correlation between continuous parameters. The strength of the correlation was considered to be more important in interpretation than were the p values, which test if $r = 0$. Strong correlation is indicated by $|r| > 0.70$, moderate if $0.5 < |r| < 0.7$, and of decreasing strength if below 0.5.

Protein intensity fold-change ratios were calculated from the RPPA intensity values. Ratios were calculated between tumors sampled prior to initiating single agent administration, after 2 weeks of single agent (2 weeks/0 weeks ratio), and after 2 weeks of dual agent administration (6 weeks/2 weeks for second drug addition and 6 weeks/0 weeks for total change over time). These ratios were median-centered and clustered using Cluster 2.0 software. Student's *t* test for differences between average protein intensity ratios at these intervals between patients in cluster 1 *versus* cluster 2 was calculated using Microsoft Excel by grouping all the ratios for individual clusters. A second analysis using Student's *t* test evaluated the ratio of signal at 6 weeks *versus* on-study to identify a core group of putative biomarkers of treatment interval. Time-to-event end points, such as progression-free survival, were computed using Kaplan-Meier statistics, with comparisons made using a log-rank test.

RESULTS

Patients and Specimens—Twenty eight patients were enrolled in the expansion translational cohort to get 10 patients with triplet biopsies (Consort diagram, Fig. 1*B*). Patient demographics, tumor characteristics, and clinical activity are shown in Table II. After final analysis, only 19 patients had three serial biopsies with at least one core per time point of adequate tissue quality and quantity for use. Reasons for incomplete biopsy sets included poor quality, fluid only, or ≤50% tumor cells (1 patient each), refusal (1), safety (2), or study removal due to toxicity or disease progression (3). Twenty six patients had adequate peripheral blood mononuclear cell ascertainment and serial monthly blood sampling (aggregate VEGF concentration results were reported (6)). Twenty three patients had all three planned [^{18}F]FDG-PET scans, and 16 patients had all planned MRs; most common causes for incomplete imaging series were obesity and claustrophobia for MR, and scheduling for out-of-town patients.

Biochemical Illustration of Mechanism—RPPA was used to confirm the presence, activation, and inhibition of select putative biochemical/predictive targets. ERK activation, the Raf kinase downstream event, was significantly reduced with 2 weeks of sorafenib but not in patients receiving bevacizumab ($p = 0.02$; Fig. 3*A*). Patients randomized to single agent bevacizumab had a lower CD31 vessel count at 2 weeks ($p = 0.05$; Fig. 3*B*), consistent with the greater activity of ligand neutralization. Increased circulating VEGF concentrations have been observed with multiple inhibitors of angiogenic signaling pathways (5, 16), and were confirmed in this patient cohort (6). Consistent with this, we found decreased tissue pERK at 2 weeks correlated with higher circulating VEGF concentration at both 2 and 6 weeks ($r = -0.60$, $p = 0.024$; $r = -0.63$, $p = 0.0501$, respectively; Table III).

Combination Therapy Results in Reduction in Vascular Flow and Metabolism—Functional imaging was used to examine metabolism and vascular flow. A trend for reduced index lesion FDG-PET SUVs at 6 weeks was seen in patients who attained a PR or had SD for ≥4 cycles ($p = 0.047$; Table III). Vascular perfusion by MR-K_{trans} increased early (2 weeks; $r = 0.72$, $p = 0.042$) in patients in whom increased VEGF staining was observed in the 6-week biopsy, a pharmacodynamic validation of the biochemical observation. Vascular permeability, k_{ep}, increased at 6 weeks in patients who had increased CD31-positive microvessels at 2 weeks ($r = 0.75$, $p = 0.02$). The increase in k_{ep} in these tumor areas could be due to increased microvessels, increased permeability of those microvessels, or both. k_{ep} was lower at the 2-week mark in patients randomized to receive sorafenib first ($p = 0.01$), suggesting that it had a detectable anti-vascular effect. Similar effects were not seen with bevacizumab; this may be in part due to imaging being done after a single dose of 5 mg/kg bevacizumab, below the doses for which functional imaging changes have been reported. These individual comparisons show the mechanism of the combination and suggest end points for further analysis.

Association with Disease Behavior—Biomarker value is based upon linkage to a pertinent clinical event. We next examined the relationship between the biochemical and pharmacodynamic findings and clinical benefit (Table III). A strong relationship between decreased p-ERK ($p = 0.011$) and p-AKT ($p = 0.015$) was seen with combination treatment in cases where significant tumor regression or necrosis was present in post-treatment biopsies. Tumors of patients who received more cycles of therapy expressed less cleaved PARP at base line ($r = -0.45$, $p = 0.053$); this might be interpreted to mean there was more viable tumor for re-

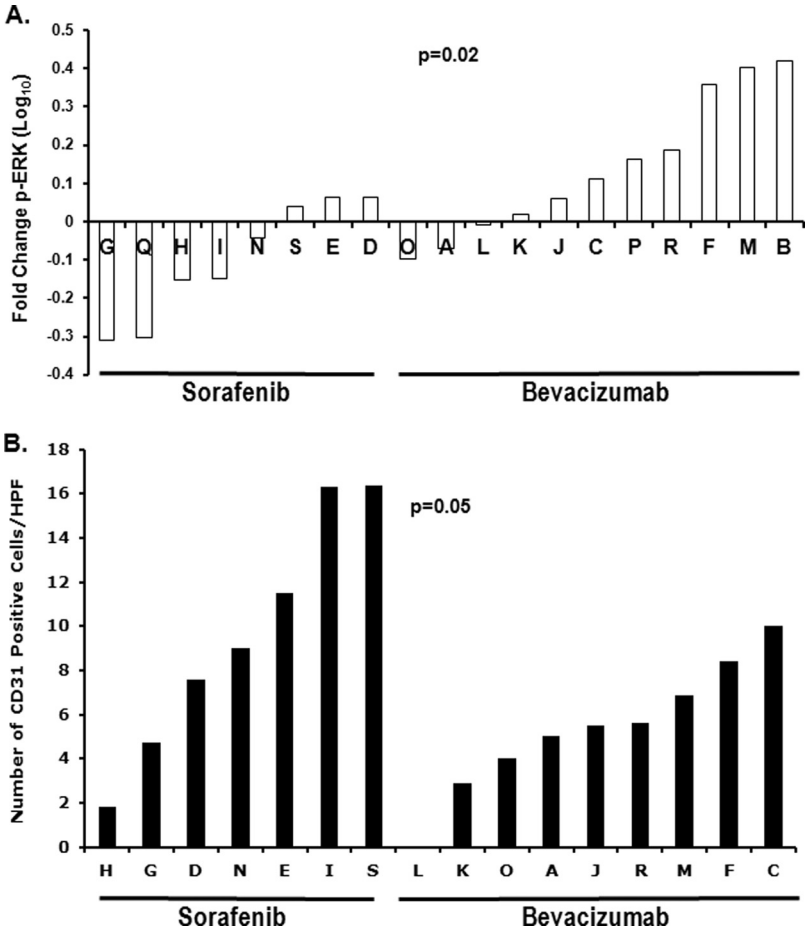

FIG. 3. **Single agent behavior of sorafenib and bevacizumab.** *A,* fold-change in activation of p-ERK in tumor protein expression occurring in patients receiving either 2 weeks of single agent sorafenib (*left group*) or bevacizumab (*right group*) is shown ($p < 0.02$). *B,* $CD31^+$ cells per high power field in tumor in patients receiving either 2 weeks of single agent sorafenib or bevacizumab is shown ($p < 0.05$).

sponse. Changes in cleaved PARP correlated with patient receipt of a greater number of cycles ($r = 0.59$; $p = 0.0072$), suggesting increased apoptosis was associated with longer progression-free intervals. Similarly, a moderate correlation was found between the early apoptosis event of change in caspase 3 cleavage ($r = 0.50$, $p = 0.03$) and decreased Ki67 staining with longer time on treatment ($r = -0.70$, $p = 0.016$), both of which would infer net tumor loss. In addition, patients receiving more cycles of therapy also had decreased levels of pVEGFR2 at baseline ($r = 0.45$, $p = 0.053$); this has also been observed in other studies suggesting that anti-angiogenic activity may be more active with moderate angiogenesis rather than robust activity. A trend was observed between decreased PET SUV values on monotherapy in patients who received more cycles ($r = -0.41$, $p = 0.044$). This suggests that PET changes at 2 weeks might be a predictive biomarker. Continued reduction in SUV values on the 6-week PET scan with combination therapy occurred in patients who had a partial response or prolonged S.D. ($p = 0.047$). Together, these findings suggest an overall inhibition of angiogenesis as the driving mechanism.

The value of a comprehensive translational data collection is the ability to examine the contribution of molecular and functional results in aggregate. We next explored the target protein changes in the patients as a grouped analysis. Unsupervised hierarchical clustering of both proteins and patients segregated into two major clusters (Fig. 4*A*). Next, the relative change in protein intensity with a single agent was compared with dual agent administration in patients from the two different clusters (Fig. 4*B*). The overall protein changes between the two groups of patients was statistically significantly different ($p = 0.00006$), with tumors from cluster 1 patients having an average decrease in protein intensity values with addition of the second agent, and an overall increase in tumors from cluster 2 patients. This difference correlated with clinical benefit, as indicated by the number of cycles each patient received (Fig. 4*C*). Patients in cluster 1, whose tumors responded to the addition of the second agent with a decrease in protein intensity, had a statistically significantly longer time on the study ($p = 0.01$) and thus progression-free survival. Within this analysis, relative to cluster 1, reduced apoptosis (decreased cleaved PARP) and reduced total BRAF, pVEGFR2, AKT, and p-endothelial nitric-oxide synthase grouped together as a potential poor outcome biomarker ($p = 0.011$; Fig. 4*D*).

Other Planned Analyses—Angiogenic potential of patient sera in a rat aortic ring assay was unrevealing (17). Tumor KRAS and BRAF mutational analysis revealed one patient with

TABLE III
Biologic end points associated with clinical parameters

Proof of mechanism endpoints	*r* value	*p* value
End point in tumor biopsies		
Decreased p-ERK with sorafenib therapy *versus* bevacizumab single agents		0.02
Decreased CD31 count with bevacizumab therapy *versus* sorafenib single agents		0.05
Decreased pERK at 2 weeks with increased circulating VEGF levels at 2 weeks[a]	−0.60	0.024
Decreased pERK at 2 weeks with increased circulating VEGF levels at 6 weeks	−0.63	0.050
Dynamic imaging end points		
Reduced PET activity in patients with PR or S.D. > 4 cycles *versus* PD		0.047
Increased vascular perfusion (K_{trans}) on DCE-MRI[a] at 2 weeks with increased VEGF in tumor biopsies at 6 weeks	0.72	0.042
Increased vascular permeability (K_{ep}) on DCE-MRI at 6 weeks with increased tumor CD31 at 2 weeks[a]	0.75	0.02
Increased vascular permeability (K_{ep}) with sorafenib treatment, first *versus* later		0.01
Decreased PET activity at 6 weeks with PR or S.D. *versus* PD		0.047
Biological end points associated with disease behavior		
Decreased p-ERK in tumor with regression/necrosis in post-treatment biopsy		0.011
Decreased p-AKT in tumor with regression/necrosis in post-treatment biopsy		0.015
Increased cleaved PARP with greater number of treatment cycles	0.59	0.0072
Increased cleaved caspase 3 at 6 weeks with increased number of cycles of therapy	0.50	0.030
Decreased Ki67 at 6 weeks with increased number of cycles of therapy	−0.70	0.016
Biologic end points associated with number of cycles of treatment		
Lower cleaved PARP at base line	−0.45	0.053
Lower p-VEGFR2 at base line	−0.45	0.053
Decreased PET activity at 2 weeks[a]	−0.41	0.044

[a] Two-week analyses were done with pooled data from both monotherapy groups to maintain analytic power.

a codon 12 KRAS mutation; this patient could not be assessed for clinical benefit due to removal from the study for uncontrolled hypertension. CYP3A4 SNP analyses yielded no significant differences between patients (18–20).

DISCUSSION

Increasingly, the therapeutic potential for targeted agent combinations is being recognized. How best to combine agents is still a quandary, as is how to select the best targeted therapies for patients with recurrent solid tumors. Illustration of target affected by molecular therapeutics, linkage of target modulation with clinical benefit, and determination of predictive utility are needed. Following our ongoing interest in targeting both the tumor and its microenvironment, we elected to combine the VEGF-neutralizing monoclonal antibody bevacizumab with the c-RAF/VEGFR2-targeted sorafenib, hypothesizing that these agents together could affect tumor cells, stromal cells, and vascular elements. To address those objectives, we incorporated serial tumor biopsies, functional imaging, and blood collections to provide biochemical and clinical measures of target effect and anti-tumor activity. The trial design, novel at the time, randomized an initial round of monotherapy for target validation, followed by continued combination therapy with which to examine potentially predictive changes. We show here that the expected targets were hit and correlated with clinical benefit, as defined by continued study treatment (treatment interval). Aggregate proteomic analysis described a panel of biochemical changes in the tumor, occurring between pretreatment and 6 weeks that statistically and significantly correlated with treatment interval. The set of end points identified in Fig. 4*D* will be examined for potential validation in prospectively collected samples in the phase II trial of sorafenib and bevacizumab in ovarian cancer patients that have recently completed accrual.

An ideal predictive biomarker is one that can be applied prior to treatment and will accurately forecast response to therapy (8, 21). They can be used for trial enrichment, patient triage, and to describe biosimilars. Incorporation in our trial of a monotherapy element and multiple translational end points, coupled with the clinical benefits observed, provided the template for predictive biomarker discovery. We validated both FDG-PET and DCE-MRI as measures of tumor vascularity in the context of sorafenib and bevacizumab treatment. Change in vascular flow as estimated by functional imaging has been shown to be predictive of the benefit of imatinib when used in gastrointestinal tumors (22), and there are reports where FDG-PET changes can be predictive of response to bevacizumab-based therapy for glioma, colorectal, and head and neck cancers (23–25). In our study, both functional imaging modalities contributed to the demonstration that the combination of sorafenib and bevacizumab affected their benefit through an anti-angiogenic drive.

Incorporation of a discovery of the proteomics component with assessment of multiple pharmacodynamic end points provided a dataset from which we could look for changes that would predict prolonged treatment intervals. Aggregate anal-

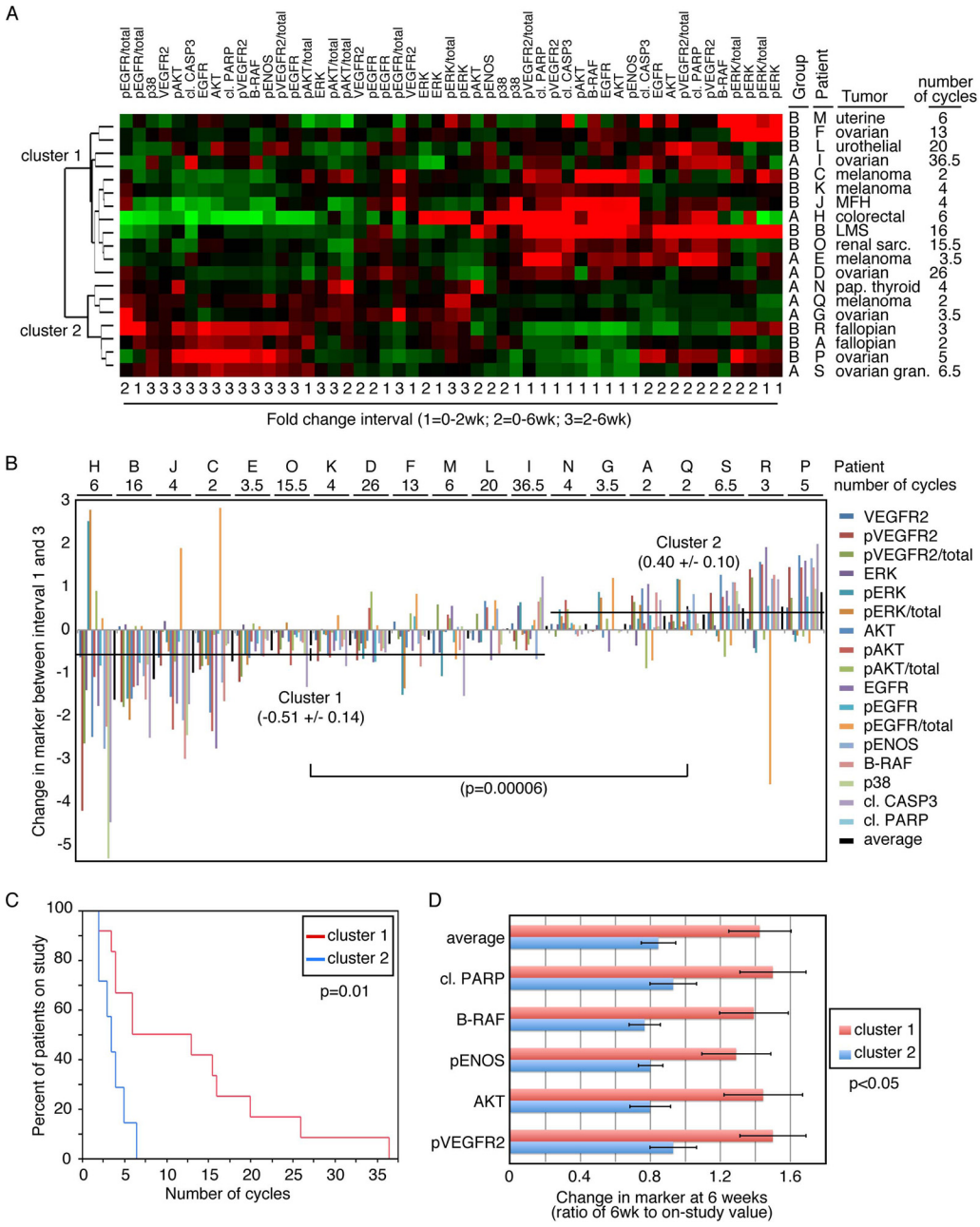

FIG. 4. **Coordinate changes in signaling predict clinical benefit.** *A,* heat map assessment of changes in signaling proteins over monotherapy (*1*), combination therapy (*2*), or the change with the addition of the second agent (*3*). Unsupervised clustering identifies two groups of patients. *B,* waterfall plot of the changes in signaling end point from monotherapy (*1*) and addition of the second agent (*3*) identifies statistically significant ($p = 0.00006$) differences between *clusters 1* and *2* from (*A*). *C,* Kaplan-Meier statistics demonstrate different clinical outcome for clusters 1 and 2 ($p = 0.01$) indicating that an increase in signaling events with addition of the second agent predicts poor performance to therapy. *D,* exploratory predictive biomarker. Further analysis of changes occurring at 6 weeks relative to on-study yielded a subset of proteomic changes that together and individually were attenuated by patients in cluster 1 who had clinical benefit and were increased in cluster 2 patients who did not respond to therapy. This identifies a potential biomarker subset for further validation.

ysis of the proteomic changes against treatment duration segregated two groups in an unsupervised clustering. Biochemical changes between pretreatment and 2-week monotherapy that clustered in group 2, the short treatment interval group, include reduction in B-RAF, pVEGFR2, total EGF receptor, and total AKT. The most striking changes, shown in Fig. 4*B*, were the relative increase in pVEGFR2 and activated VEGFR2 ratio, activated AKT ratio, pENOS, pEGFR, and total AKT and EGF receptor upon addition of the second agent in the short treatment interval cohort. This suggests that addition of the second agent might be antagonistic rather than positively interactive. Further characterizing and validating

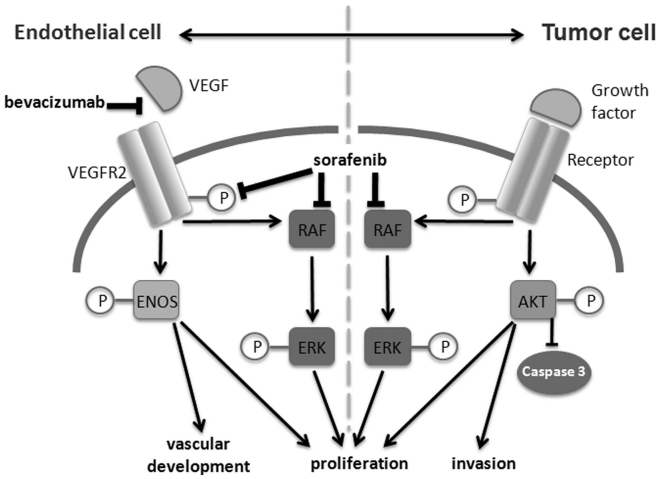

FIG. 5. **Pathway.** Pathways in the endothelial cell and tumor cell show the interactive effects of the combination of sorafenib and bevacizumab on their different target cells.

this potential negative biomarker group could be equally important to moving agents such as these forward in combinations.

It is unclear whether we can improve clinical benefit by using targeted agents in series (vertically) or in parallel (horizontally). This study incorporated putative interactions in both directions, VEGF/VEGFR2 and VEGF/c-RAF, that were then queried as to target inhibition and for predictive value in the aggregate analysis (Fig. 5). Biochemical parameters differed with single agent therapy; those differences were lost and broader overlapping signal inhibition was observed upon the combination of the two agents. This breadth of altered regulation by the combination could, in part, explain the increase in toxicity and also the clinical benefit seen with the addition of bevacizumab to sorafenib. Hand-foot syndrome, a recognized sorafenib toxicity, was increased in frequency with addition of bevacizumab and then further increased when bevacizumab dose increased. Furthermore, there is a possibility of increasing value of an otherwise minimally active drug when used in a rational biochemical combination. The 19 ovarian cancer patients treated on this phase 1 trial had a 47% response rate with a progression free survival median of 6 months (mean, 11 months; range 4–37) (7). Other studies incorporating single agent bevacizumab in recurrent ovarian cancer patients had response rates ranging from 16 to 21% with median duration of 4.4–4.7 months (26, 27), and single agent sorafenib has limited activity in ovarian cancer (28, 29).

Identification of predictive biomarkers for anti-angiogenic therapy is a critical need. Approaches taken to date have included genomic and genetic studies, and proteomic studies at the serologic and tissue levels, as in our study. Several investigators have suggested that SNPs in the VEGF pathway genes may have predictive value. Recently, Lambrechts *et al.* (30) evaluated SNPs in the VEGF pathway in a subset of samples from the randomized placebo-controlled trials, AViTA (BO17706) and AVOREN (BO17705), randomizing ± bevacizumab for gemcitabine/erlotinib in pancreatic cancer and interferon α2a for renal cell carcinoma, respectively. Their discovery phase identified a synonymous SNP affecting Tyr^{1213}-VEGFR1 in its tyrosine kinase domain as associated with progression-free survival in the bevacizumab group (HR 2.1; $p = 0.00014$); this was validated independently as predictive in the progression-free survival of the bevacizumab group in AVOREN (HR 1.81, $p = 0.033$). This SNP increased VEGFR1 expression and downstream VEGFR1 signaling. Serologic proteomics has been applied by several groups. Prespecified serologic end points were analyzed in the AVAGAST randomized placebo-controlled trial of the role of bevacizumab with cisplatin/capecitabine therapy for advanced gastric cancer. They show that high pretreatment circulating concentrations of VEGF-A and low pretreatment circulating neuropilin-1 were prognostic for improved survival (HR 0.7) (31). A similar survival prognostic, but not predictive, value was observed for VEGF-A concentrations in a series of other studies of bevacizumab ± chemotherapy in solid tumors (32, 33). Angiome profiling was also done in a gemcitabine ± bevacizumab-randomized trial (CALGB 80303) identifying a different survival prognostic signature in the bevacizumab *versus* placebo arms, both of which included IGFBP1 and PDGF-AA (34). Our study is the first to look at a broad array of activated protein end points over time in tumor tissue from which to develop hypothesis-generating predictive angio-biomarkers.

Illustration of biochemical mechanism and identification of predictive biomarkers remain a challenge. Biomarkers can be genetic, epigenetic, and/or proteomic, and investigators must balance advantages and disadvantages of the multiple analysis platforms for each. We focused on the RPPA format to assess biomarkers at the protein level, where the effects of genetic, epigenetic, and post-translational modifications coalesce to truly affect cellular function. We applied our previously reported RPPA optimization methods and controls (15). Using an approach containing monotherapy and serially sampled translational end points, we confirmed on-target activity of activated ERK for sorafenib, and microvessel density as a marker of tumor vascular response for bevacizumab. Although neither result was unexpected, the analysis indicated that the biological effect of the combination was not broadly against tumor, stroma, and vascular elements as hypothesized, but prominently against the vasculature defining this as a true anti-angiogenic combination. End point analysis identified a panel of biochemical changes measured in the tumor tissue that correlated significantly with clinical benefit to the combination. This biomarker panel will be examined prospectively as a potential predictive biomarker change in the ongoing phase II study of sorafenib and bevacizumab in ovarian cancer NCT00436215. The ever-increasing classes of targeted agents available for single and combination studies preclude examination of every possible combination. Currently, rational combina-

tions must be designed based upon cellular target, interactive biochemical and/or biological targets, and toxicity profiles. This is an example where target, inhibition, and outcome harmonized in a tolerable and active regimen.

Acknowledgments—We thank Drs. John Wright and Helen Chen from the Cancer Therapy Evaluation Program, NCI, National Institutes of Health, for their input during the clinical trial.

* This work was supported, in whole or in part, by National Institutes of Health Intramural Program of the Center for Cancer Research, the NCI, the Nuclear Medicine Department, National Institutes of Health Clinical Center, and the Center for Interventional Oncology, Radiology, and Imaging Sciences.

[b] The authors contributed equally to this work.

[e] Supported by the John and Inger Fredriksen Ovarian Cancer Foundation.

[i] Supported by the ASCO Foundation/Conquer Cancer Foundation Young Investigator Award (to N.A.).

[m] To whom correspondence should be addressed: National Institutes of Health, 10 Center Dr. MSC 1906, Bethesda, MD 20892. Tel.: 301-402-2726; Fax: 301-480-5142; E-mail: kohne@mail.nih.gov.

REFERENCES

1. Wilson, P. M., LaBonte, M. J., and Lenz, H. J. (2013) Assessing the *in vivo* efficacy of biologic antiangiogenic therapies. *Cancer Chemother. Pharmacol.* **71,** 1–12
2. Chen, H. X. (2004) Expanding the clinical development of bevacizumab. *Oncologist* **9,** 27–35
3. Heath, V. L., and Bicknell, R. (2009) Anticancer strategies involving the vasculature. *Nat. Rev. Clin. Oncol.* **6,** 395–404
4. Teoh, D. G., and Secord, A. A. (2011) Antiangiogenic therapies in epithelial ovarian cancer. *Cancer Control* **18,** 31–43
5. Kelly, R. J., Sharon, E., and Hassan, R. (2011) Chemotherapy and targeted therapies for unresectable malignant mesothelioma. *Lung Cancer* **73,** 256–263
6. Azad, N. S., Posadas, E. M., Kwitkowski, V. E., Steinberg, S. M., Jain, L., Annunziata, C. M., Minasian, L., Sarosy, G., Kotz, H. L., Premkumar, A., Cao, L., McNally, D., Chow, C., Chen, H. X., Wright, J. J., Figg, W. D., and Kohn, E. C. (2008) Combination targeted therapy with sorafenib and bevacizumab results in enhanced toxicity and antitumor activity. *J. Clin. Oncol.* **26,** 3709–3714
7. Lee, J. M., Sarosy, G. A., Annunziata, C. M., Azad, N., Minasian, L., Kotz, H., Squires, J., Houston, N., and Kohn, E. C. (2010) Combination therapy: intermittent sorafenib with bevacizumab yields activity and decreased toxicity. *Br. J. Cancer* **102,** 495–499
8. Lee, J.-M., Han, J. J., Altwerger, G., and Kohn, E. C. (2011) Proteomics and biomarkers in clinical trials for drug development. *J. Proteomics* **74,** 2632–2641
9. McDonald, D. M., and Choyke, P. L. (2003) Imaging of angiogenesis: from microscope to clinic. *Nat. Med.* **9,** 713–725
10. Turkbey, B., Kobayashi, H., Ogawa, M., Bernardo, M., and Choyke, P. L. (2009) Imaging of tumor angiogenesis: functional or targeted? *AJR Am. J. Roentgenol.* **193,** 304–313
11. Choyke, P. L., Dwyer, A. J., and Knopp, M. V. (2003) Functional tumor imaging with dynamic contrast-enhanced magnetic resonance imaging. *J. Magn. Reson. Imaging* **17,** 509–520
12. Kety, S. S. (1951) The theory and applications of the exchange of inert gas at the lungs and tissues. *Pharmacol. Rev.* **3,** 1–41
13. Annunziata, C. M., Walker, A. J., Minasian, L., Yu, M., Kotz, H., Wood, B. J., Calvo, K., Choyke, P., Kimm, D., Steinberg, S. M., and Kohn, E. C. (2010) Vandetanib, designed to inhibit VEGFR2 and EGFR signaling, had no clinical activity as monotherapy for recurrent ovarian cancer and no detectable modulation of VEGFR2. *Clin. Cancer Res.* **16,** 664–672
14. Winters, M., Dabir, B., Yu, M., and Kohn, E. C. (2007) Constitution and quantity of lysis buffer alters outcome of reverse phase protein microarrays. *Proteomics* **7,** 4066–4068
15. Kim, G., Davidson, B., Henning, R., Wang, J., Yu, M., Annunziata, C., Hetland, T., and Kohn, E. C. (2012) Adhesion molecule protein signature in ovarian cancer effusions is prognostic of patient outcome. *Cancer* **118,** 1543–1553
16. Zurita, A. J., Jonasch, E., Wang, X., Khajavi, M., Yan, S., Du, D. Z., Xu, L., Herynk, M. H., McKee, K. S., Tran, H. T., Logothetis, C. J., Tannir, N. M., and Heymach, J. V. (2012) A cytokine and angiogenic factor (CAF) analysis in plasma for selection of sorafenib therapy in patients with metastatic renal cell carcinoma. *Ann. Oncol.* **23,** 46–52
17. Gardner, E. R., Kelly, M., Springman, E., Lee, K. J., Li, H., Moore, W., and Figg, W. D. (2012) Antiangiogenic and antitumor activity of LP-261, a novel oral tubulin-binding agent, alone and in combination with bevacizumab. *Invest. New Drugs* **30,** 90–97
18. Jain, L., Sissung, T. M., Danesi, R., Kohn, E. C., Dahut, W. L., Kummar, S., Venzon, D., Liewehr, D., English, B. C., Baum, C. E., Yarchoan, R., Giaccone, G., Venitz, J., Price, D. K., and Figg, W. D. (2010) Hypertension and hand-foot skin reactions related to VEGFR2 genotype and improved clinical outcome following bevacizumab and sorafenib. *J. Exp. Clin. Cancer Res.* **29,** 95
19. Jain, L., Woo, S., Gardner, E. R., Dahut, W. L., Kohn, E. C., Kummar, S., Mould, D. R., Giaccone, G., Yarchoan, R., Venitz, J., and Figg, W. D. (2011) Population pharmacokinetic analysis of sorafenib in patients with solid tumours. *Br. J. Clin. Pharmacol.* **72,** 294–305
20. Peer, C. J., Sissung, T. M., Kim, A., Jain, L., Woo, S., Gardner, E. R., Kirkland, C. T., Troutman, S. M., English, B. C., Richardson, E. D., Federspiel, J., Venzon, D., Dahut, W., Kohn, E., Kummar, S., Yarchoan, R., Giaccone, G., Widemann, B., and Figg, W. D. (2012) Sorafenib is an inhibitor of UGT1A1 but is metabolized by UGT1A9: implications of genetic variants on pharmacokinetics and hyperbilirubinemia. *Clin. Cancer Res.* **18,** 2099–2107
21. Tan, D. S., Thomas, G. V., Garrett, M. D., Banerji, U., de Bono, J. S., Kaye, S. B., and Workman, P. (2009) Biomarker-driven early clinical trials in oncology: a paradigm shift in drug development. *Cancer J.* **15,** 406–420
22. Van den Abbeele, A. D. (2008) The lessons of GIST–PET and PET/CT: a new paradigm for imaging. *Oncologist* **13,** 8–13
23. Bertolini, F., Malavasi, N., Scarabelli, L., Fiocchi, F., Bagni, B., Del Giovane, C., Colucci, G., Gerunda, G. E., Depenni, R., Zironi, S., Fontana, A., Pettorelli, E., Luppi, G., and Conte, P. F. (2011) FOLFOX6 and bevacizumab in non-optimally resectable liver metastases from colorectal cancer. *Br. J. Cancer* **104,** 1079–1084
24. Chen, W., Delaloye, S., Silverman, D. H., Geist, C., Czernin, J., Sayre, J., Satyamurthy, N., Pope, W., Lai, A., Phelps, M. E., and Cloughesy, T. (2007) Predicting treatment response of malignant gliomas to bevacizumab and irinotecan by imaging proliferation with [^{18}F]fluorothymidine positron emission tomography: a pilot study. *J. Clin. Oncol.* **25,** 4714–4721
25. Jansen, J. F., Schöder, H., Lee, N. Y., Stambuk, H. E., Wang, Y., Fury, M. G., Patel, S. G., Pfister, D. G., Shah, J. P., Koutcher, J. A., and Shukla-Dave, A. (2012) Tumor metabolism and perfusion in head and neck squamous cell carcinoma: pretreatment multimodality imaging with ^{1}H magnetic resonance spectroscopy, dynamic contrast-enhanced MRI, and [^{18}F]FDG-PET. *Int. J. Radiat. Oncol. Biol. Phys.* **82,** 299–307
26. Burger, R. A. (2007) Experience with bevacizumab in the management of epithelial ovarian cancer. *J. Clin. Oncol.* **25,** 2902–2908
27. Cannistra, S. A., Matulonis, U. A., Penson, R. T., Hambleton, J., Dupont, J., Mackey, H., Douglas, J., Burger, R. A., Armstrong, D., Wenham, R., and McGuire, W. (2007) Phase II study of bevacizumab in patients with platinum-resistant ovarian cancer or peritoneal serous cancer. *J. Clin. Oncol.* **25,** 5180–5186
28. Bodnar, L., Górnas, M., and Szczylik, C. (2011) Sorafenib as a third line therapy in patients with epithelial ovarian cancer or primary peritoneal cancer: A phase II study. *Gynecol. Oncol.* **123,** 33–36
29. Matei, D., Sill, M. W., Lankes, H. A., DeGeest, K., Bristow, R. E., Mutch, D., Yamada, S. D., Cohn, D., Calvert, V., Farley, J., Petricoin, E. F., and Birrer, M. J. (2011) Activity of sorafenib in recurrent ovarian cancer and primary peritoneal carcinomatosis: a gynecologic oncology group trial. *J. Clin. Oncol.* **29,** 69–75
30. Lambrechts, D., Claes, B., Delmar, P., Reumers, J., Mazzone, M., Yesilyurt, B. T., Devlieger, R., Verslype, C., Tejpar, S., Wildiers, H., de Haas, S., Carmeliet, P., Scherer, S. J., and Van Cutsem, E. (2012) VEGF pathway genetic variants as biomarkers of treatment outcome with bevacizumab: an analysis of data from the AViTA and AVOREN randomised trials. *Lancet Oncol.* **13,** 724–733

31. Van Cutsem, E., de Haas, S., Kang, Y. K., Ohtsu, A., Tebbutt, N. C., Ming Xu, J., Peng Yong, W., Langer, B., Delmar, P., Scherer, S. J., and Shah, M. A. (2012) Bevacizumab in combination with chemotherapy as first-line therapy in advanced gastric cancer: a biomarker evaluation from the AVAGAST randomized phase III trial. *J. Clin. Oncol.* **30,** 2119–2127
32. Hegde, P. S., Jubb, A. M., Chen, D., Li, N. F., Meng, Y. G., Bernaards, C., Elliott, R., Scherer, S. J., Chen, D. S. (2013) Predictive Impact of Circulating Vascular Endothelial Growth Factor in Four Phase III Trials Evaluating Bevacizumab. *Clin Cancer Res.* **19,** 929–937
33. Bates, D. O., Catalano, P. J., Symonds, K. E., Varey, A. H., Ramani, P., O'Dwyer, P. J., Giantonio, B. J., Meropol, N. J., Benson, A. B., and Harper, S. J. (2012) Association between VEGF splice isoforms and progression-free survival in metastatic colorectal cancer patients treated with Bevacizumab. *Clin. Cancer Res.* **18,** 6384–6391
34. Nixon, A. B., Pang, H., Starr, M., Hollis, D., Friedman, P. N., Bertagnolli, M. M., Kindler, H. L., Goldberg, R. M., Venook, A. P., and Hurwitz, H. (2011) Prognostic and predictive blood-based biomarkers in patients with advanced pancreatic cancer: Results from CALGB 80303. *J. Clin. Oncol.* **29,** Suppl. (Abstr. 10508)